AIAA JOURNAL
Vol. 34, No. 8, August 1996

Effect of Ply-Drop Configuration on Delamination Strength of Tapered Composite Structures

Anthony D. Botting,* Anthony J. Vizzini,† and Sung W. Lee‡
University of Maryland, College Park, Maryland 20742-3015

Delamination suppression by altering the sequence of ply drops is evaluated for tapered glass/epoxy laminates. Two different stacking sequences with thin section layups of $[0_4/\pm 45_2]_s$ and $[\pm 45_2/0_4]_s$ containing drops of three sets of ±45-deg plies are investigated. A finite element model using three-dimensional solid elements is constructed to evaluate the state of interlaminar stress in and around the ply drops. The effect of the stress-free edge is considered by providing a mesh refinement near the free edge. Tapered specimens are manufactured and tested under quasistatic uniaxial tension. For specimens of $[0_4/\pm 45_2]_s$ stacking sequence, delamination strength is dependent on the ply-drop sequence, and structural tailoring of the ply drop region results in a reduced interlaminar stress state and an associated increase in delamination strength. Structural tailoring, however, appears to be ineffective in the $[\pm 45_2/0_4]_s$ specimens. The measured delamination strengths are insensitive to the ply-drop sequence, although the finite element model indicates a stronger sensitivity. In general, the finite element model correlates well with the data. The measured differences in strength among the $[0_4/\pm 45_2]_s$ specimens and the overall strength difference between the $[0_4/\pm 45_2]_s$ and the $[\pm 45_2/0_4]_s$ specimens are predicted by the finite element model using strength criteria on the stress state in the interply resin region.

Introduction

A TAPER in thickness of structural components poses specific problems in applications using laminated composite materials. A reduction of thickness is effected by the termination of one or more plies. For example, to allow for blade flap, hingeless rotors require flexbeams with significant thickness changes to reduce the bending stiffness away from the hub. Often the taper region is a weak link reducing the overall load capacity of the flexbeam. Under applied loads, interlaminar stresses arise within the taper and result in delamination.[1] Once delamination has occurred, the structural integrity and the performance of the flexbeam is reduced.[2]

Tapered elements have been modeled and tested to the extent that a basic understanding of the failure mechanisms has been developed.[3–6] Researchers have concentrated on determining the state of interlaminar stress at and near the root of the taper and the strain energy release rates associated with delamination within the taper region. The knowledge base continues to be extended as researchers develop approximate analytical methods[7] and investigate the effect of cyclic loadings.[8]

One area of extreme importance is the design of the taper itself. The overall elastic response of the flexbeam, both axial and flexural, is dominated by the laminate in the thick and thin regions. Yet the strength of the flexbeam is dependent on the strength of the tapered region. By designing the taper region, the structural integrity of the flexbeam can be altered with little or no effect on its overall elastic response. Two approaches are commonly used to increase structural integrity: increase the strength of the weak link or decrease the stress state that excites the governing failure mechanism. In the case of delamination, the weak link is the interface between plies, and the contributing stress state is comprised of interlaminar stresses. A method of improving the interfacial strength, with an additional benefit of reducing the stress state, is the introduction of film adhesive. This is an effective means to delay or prevent the occurrence of free-edge delamination, as well as means to arrest delamination growth in flat laminates.[9–11] This method has also been applied to tapered laminates with varying success.[12] Delamination onset was delayed by 14% in $[\pm 45_2/0_4]_s$ tapered laminates but not in $[0_4/\pm 45_2]_s$ tapered laminates.

The second general approach to delay the occurrence of delamination initiation is to modify the interlaminar stress state at its critical location. Because the stress state near the root of the taper is considered to be the most critical, alteration near the root is sought. For example, the effect of dispersing the ply drops in 0-deg unidirectional tapered specimens was considered in Ref. 13. Unidirectional plies were used to eliminate the stiffness mismatch at the stress-free edge and, thus, eliminate the stresses that normally arise and interact with the interlaminar stresses due to the taper.

The objective of the present study is to examine through finite element analysis the stress state in tapered laminates with different ply-drop configurations. In addition, comparisons will be made with experimentally observed strengths by applying failure criteria. Three ply-drop configurations are investigated involving different sequences of ply drops. The stacking sequence is not unidirectional. Indeed, ply angles of ±45 deg are used for the dropped plies and for either the belt or core plies. The increases the effect of interlaminar stresses at the free edge. To better capture this effect, the finite element model includes a mesh refinement at the stress-free edge.

Tapered Specimen

A typical tapered laminate configuration is shown in Fig. 1. The component consists of plies that are continuous and plies that are terminated. The continuous plies can be divided further into core plies, those that are at a constant distance from the centerline along the length of the specimen, and belt plies, those that are of varying distance. In this conventional configuration, called staircase, the belt and core plies comprise sublaminates that surround the dropped plies. The plies are terminated in groups of two at regular intervals to effect the taper.

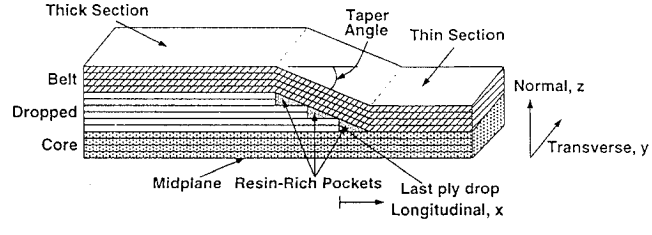

Fig. 1 Schematic drawing of tapered specimen.

Received Feb. 2, 1995; revision received Aug. 25, 1995; accepted for publication Aug. 28, 1995.

*Graduate Research Assistant, Composites Research Laboratory, Department of Aerospace Engineering.

†Associate Professor, Composites Research Laboratory, Department of Aerospace Engineering. Associate Fellow AIAA.

‡Professor, Composites Research Laboratory, Department of Aerospace Engineering. Associate Fellow AIAA.

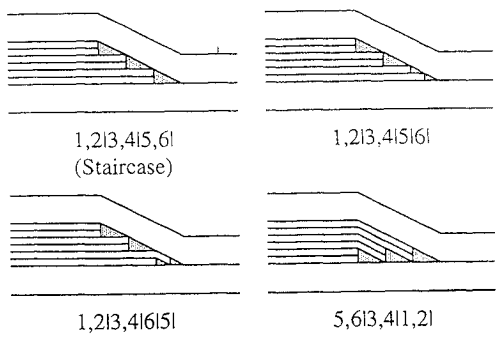

Fig. 2 Schematic drawings of alternate ply-drop sequences.

The standard staircase configuration (1, 2|3, 4|5, 6|) and the three alternate configurations considered in this paper are shown in Fig. 2. The symbol | is used to designate the dropping of a ply or plies. In the first alternate configuration, the last ply drop is spread out to reduce the effect of the discontinuity. The ply that is farther from the centerline is dropped at the conventional location, whereas the other ply is dropped halfway between the root of the taper and the conventional ply-drop location. This configuration is denoted as 1, 2|3, 4|5|6|. A variation of this configuration reverses the order of dropped plies and is denoted as 1, 2|3, 4|6|5|. The third alternate reverses the order of all of the dropped plies and is denoted as 5, 6|3, 4|1, 2|. This configuration moves the resin regions between the dropped plies and the core plies. In all cases the plies are dropped at the appropriate locations to maintain a constant change in thickness in the taper region.

In this investigation, the x axis coincides with the longitudinal direction, the y axis with the transverse direction, and the z axis with the normal direction as shown in Fig. 1. The tapered section is centered at the halfway point of the length of the specimen, and the taper angle is 5.71 deg, which results in a 10-to-1 taper ratio. The symmetric tapered laminate contains three sets of ply drops (±45-deg angle plies) nominally equidistant from each other. The ply drops are covered (top and bottom) with four plies making the total number of plies 28 in the thick section and 16 in the thin section. The stacking sequence in the thick sections are $[0_4/\pm 45_3/\pm 45_2]_s$ and $[\pm 45_2/\pm 45_3/0_4]_s$; however, the laminates are referred to by their thin section stacking sequences, $[0_4/\pm 45_2]_s$ and $[\pm 45_2/0_4]_s$, respectively.

Finite Element Analysis

The axis system used in the finite element model is depicted in Fig. 1. The origin is located at the site of the last ply drop in the standard configuration along the stress-free edge at the midplane. This location is maintained for the other configurations. The global x–z plane is shown with the y axis projecting into the plane of the page. Because of the symmetry about the x–y plane, only one-half of the laminate is modeled. There are 14 plies in the thick end that taper down to 8 plies in the thin end. The thick and thin ends of the model are located far enough from the taper area so that effects due to dropping plies are minimized. This was verified by assuring that the in-plane ply stresses and strains in the thin and thick sections are equivalent to those predicted by laminated plate theory for an equivalent flat plate under uniaxial load.

Each of the plies in the model is represented by one solid finite element in the normal direction, one or eight elements in the transverse direction, and a row of elements in the longitudinal direction. Of the eight elements in the width, the four nearest the stress-free edge are $1t_{\text{ply}}$ wide. This provides some refinement to capture the interlaminar stresses due to the stress-free edge. The next three elements are 6, 30, and $50.3t_{\text{ply}}$ wide. These seven elements represent half of the overall specimen width. The eighth element is $95.3t_{\text{ply}}$ and constitutes the other half of the width. Thin interlaminar resin layers are included between the dropped plies and the belt and core plies to increase the accuracy of the model.[12] For each configuration with eight elements in the transverse direction, there are a total of 4,360 three-dimensional elements resulting in 16,119 degrees of freedom. All of the elements except 72 are eight-node, 24-degree-of-freedom assumed stress hybrid elements. The other elements are six-node isoparametric triangular prism elements

Table 1 Material properties

SP-250-S29 glass/epoxy unidirectional tape:	
Extensional moduli, GPa	$E_L = 48.3$ $E_T = 14.5$ $E_N = 14.5$
Shear moduli, GPa	$G_{LT} = 5.5$ $G_{TN} = 4.8$ $G_{NL} = 5.5$
Poisson's ratios	$\nu_{LT} = 0.26$ $\nu_{LN} = 0.26$ $\nu_{TN} = 0.50$
Ply thickness, mm	$t_{\text{ply}} = 0.20$
Resin	
Young's modulus, GPa	$E = 3.9$
Shear modulus, GPa	$G = 1.0$
Poisson's ratio	$\nu = 0.37$
Interply resin thickness, mm	$t_{\text{resin}} = 0.020$

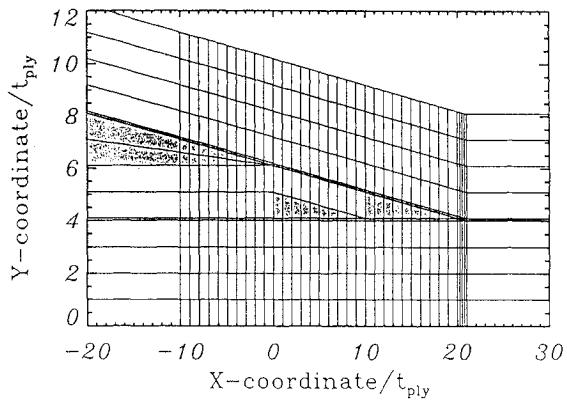

Fig. 3 Typical fine mesh used in ply-drop configurations.

that are used for the tips of the resin-rich pockets at each location of a ply drop and where the resin layers merge. A fine mesh of 30 elements in the longitudinal direction is used that extends 10 elements to the left (decreasing x) of the last ply drop and 20 elements to the right (increasing x). A portion of the model at the last ply drop for the 1, 2|3, 4|6|5| configuration is shown in Fig. 3. The thickness of the ply, t_{ply}, is assumed to be 0.200 mm (the measured nominal ply thickness from the experimental portion of this study), and the thickness of the resin rich interply layers is assumed to be 0.020 mm. The element lengths range from $1.0t_{\text{ply}}$ near the ply drop to $127.1t_{\text{ply}}$ in regions far away from the taper. The overall length of the model is 164.6 mm or $823t_{\text{ply}}$. The model width is 38.1 mm or $190.5t_{\text{ply}}$. The resin is assumed to be isotropic and the plies to be orthotropic. The material properties used are listed in Table 1.

The analysis is conducted, for each respective laminate and ply-drop sequence, by fixing the thick end and applying a uniform displacement at the thin end. The axial stress that occurs at the thin end is determined. The solution is then scaled so that an average uniaxial tensile stress of 1.0 MPa is applied over the cross section of the thin end of the laminate.

The interlaminar stresses σ_{zz}, σ_{xz}, and σ_{yz} are determined in the region near the last ply drop (delamination onset site). In the elements that are at an angle with respect to the longitudinal axis of the specimen, the stresses are rotated so that they are in terms of the local coordinate system where the x and y axes are in the plane of the ply.

Typical analytical results are presented in Figs. 4 and 5 for the standard staircase ply-drop configuration and in Figs. 6 and 7 for the two configurations that result in the greatest reduction in the stress state. In all of the figures, all six stresses are shown near the stress-free edge ($y/t_{\text{ply}} = 0$) and indicate the three-dimensional nature of the load transfer. This finite element analysis indicates that for the same applied load, the maximum von Mises stress (or maximum shear stress) in the $[\pm 45_2/0_4]_s$ laminates are lower than those in the $[0_4/\pm 45_2]_s$ laminates. This indicates that the $[\pm 45_2/0_4]_s$ laminates have in general higher strength than the $[0_4/\pm 45_2]_s$ laminates. Experimental results support this general trend.

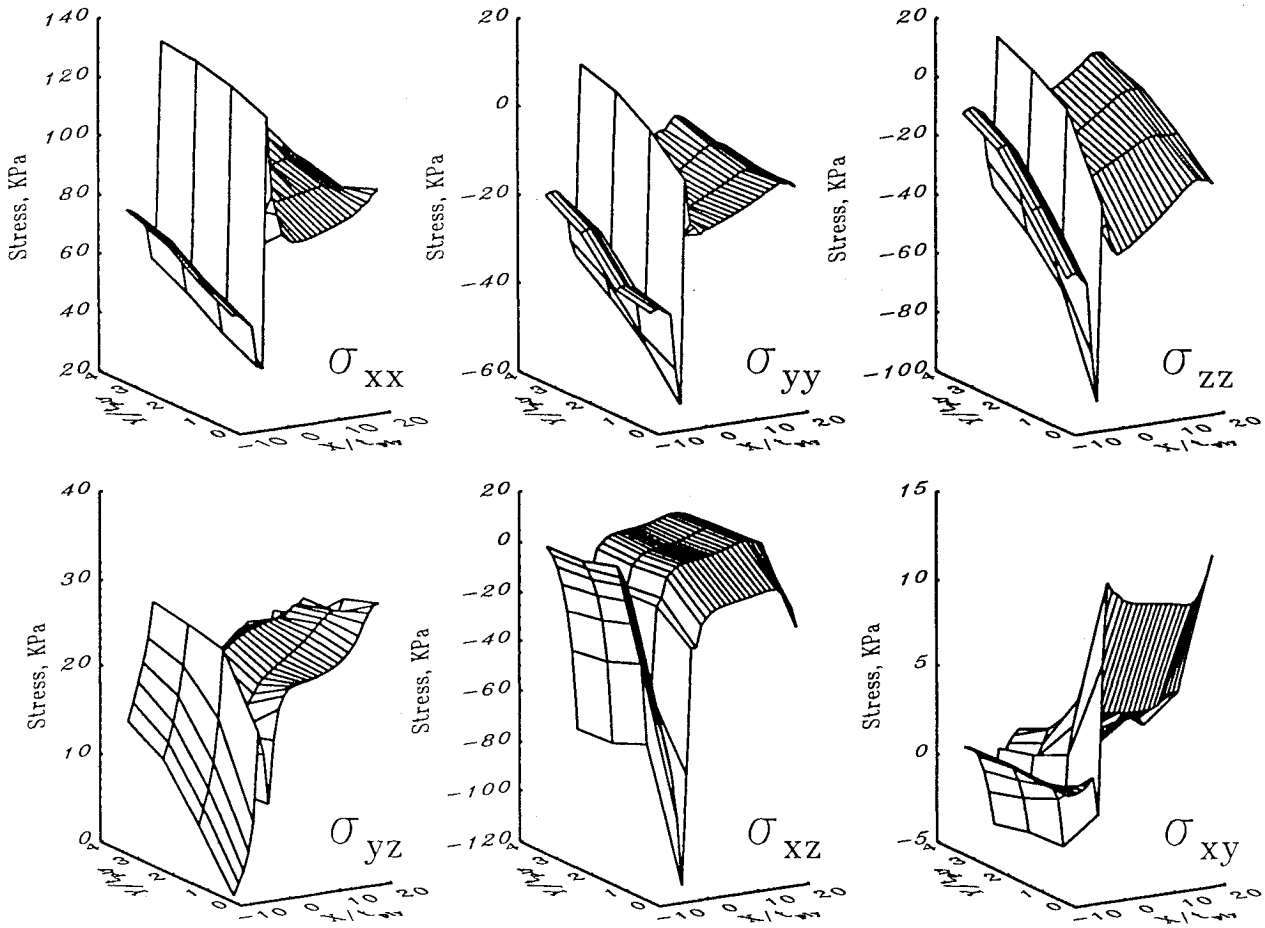

Fig. 4 Stresses in bottom resin layer of a $[0_4/\pm 45_2]_s$ tapered laminate with a standard drop configuration.

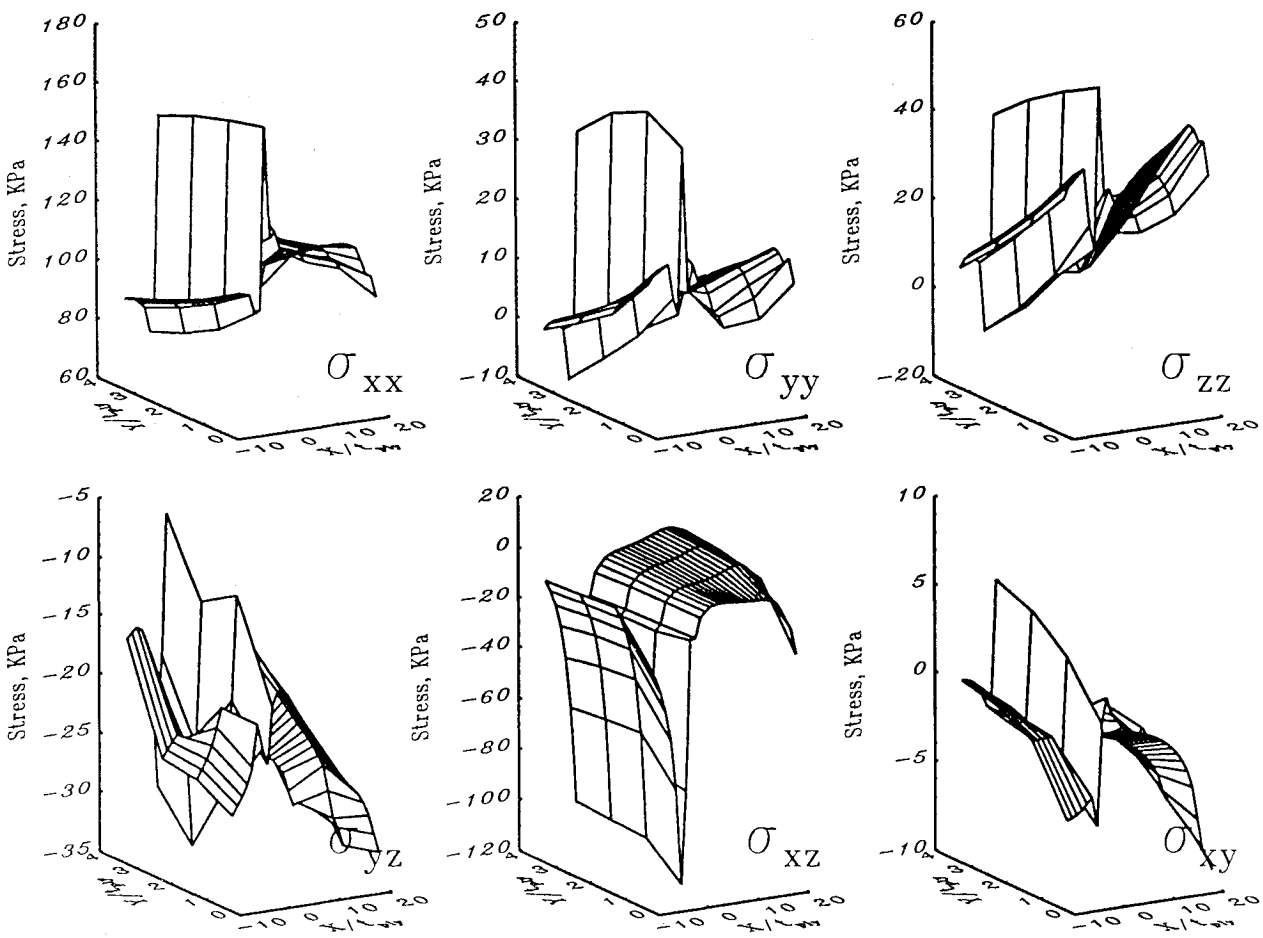

Fig. 5 Stresses in bottom resin layer of a $[\pm 45_2/0_4]_s$ tapered laminate with a standard drop configuration.

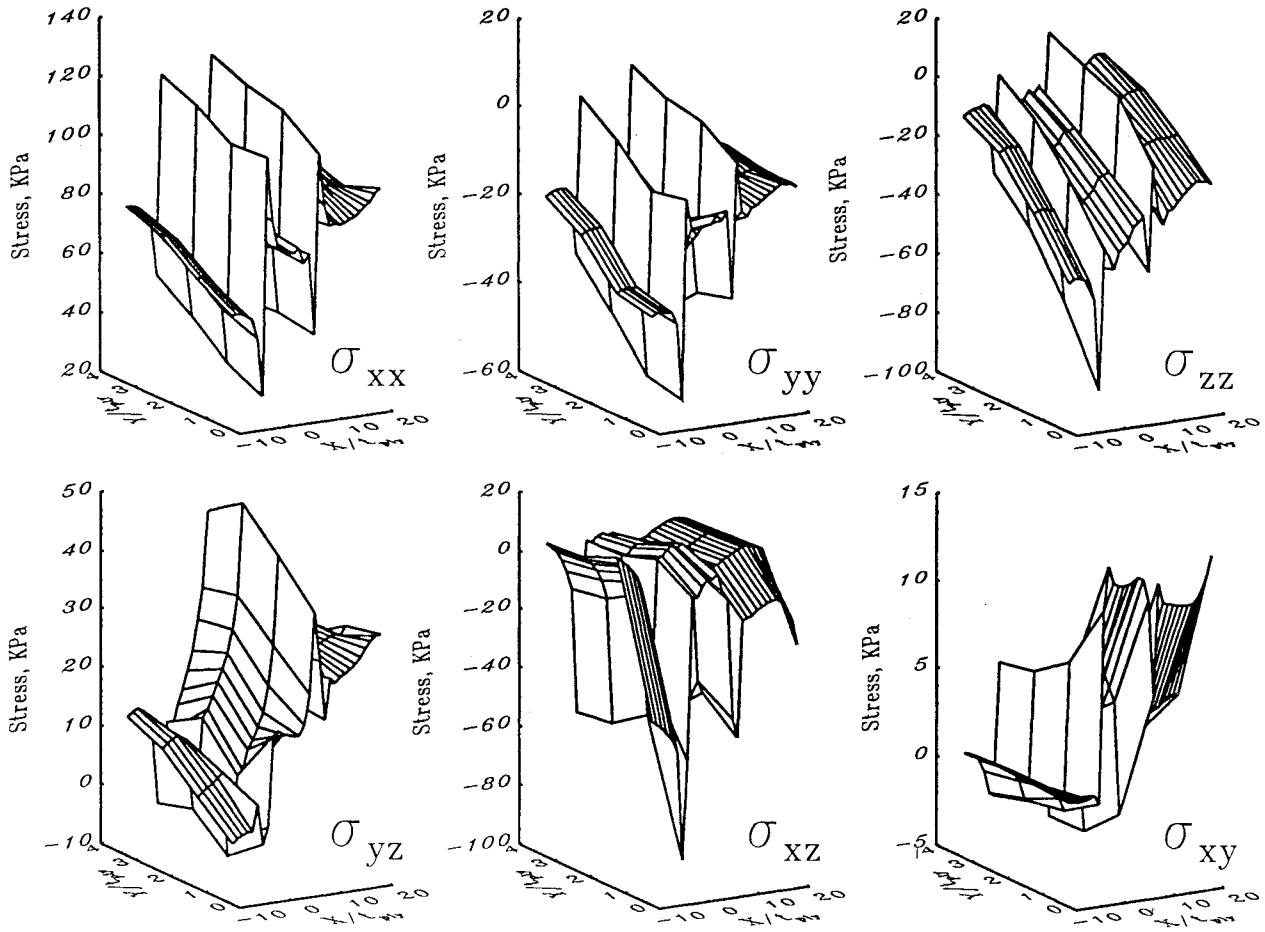

Fig. 6 Stresses in bottom resin layer of a $[0_4/\pm 45_2]_s$ tapered laminate with a (1, 2|3, 4|6|5) drop configuration.

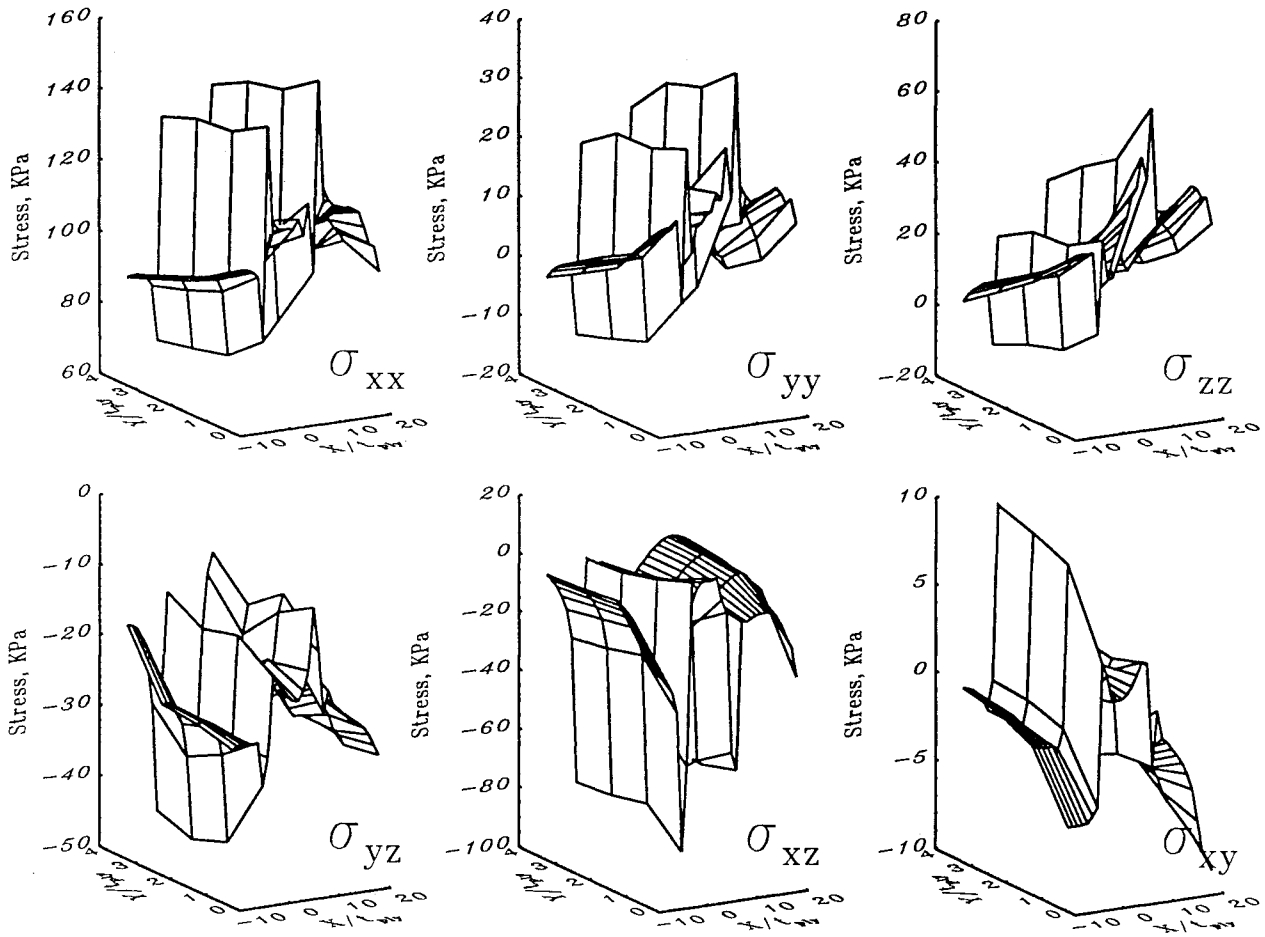

Fig. 7 Stresses in bottom resin layer of a $[\pm 45_2/0_4]_s$ tapered laminate with a (1, 2|3, 4|6|5) drop configuration.

The effect of dropping the last set of plies individually are to create a second site for interlaminar stresses to rise and to reduce the magnitude of the interlaminar stresses at the original site. Reversing the order of the plies (5, 6|3, 4|1, 2|) does not significantly affect the magnitude of the interlaminar stress state at the last ply drop. It was considered in this study because it moves the resin pockets from between the dropped and belt plies to between the dropped and core plies.

Experimental Program

A total of 48 specimens were manufactured from S-glass/epoxy, SP250-S29, unidirectional preimpregnated tape manufactured by 3M. The 305-mm-wide tape was cut with razor blades into plies to form a 305-mm wide by 280-mm long tapered laminate. The plies corresponding to the three ply drops were then cut from the ±45 deg angle plies to their respective lengths. Each half of the laminate was carefully laid up, and the two halves were joined forming one symmetric laminate.

Once the layup had been completed, the laminates were readied for the cure cycle. The laminates were placed between jig plates specially milled to the precise dimensions of the tapered component. The alignment of the jig plates was assured with three alignment pins. The necessary cure materials were also placed between the jig plates. The entire assembly was cured in an autoclave following the manufacturer's recommended cure cycle. Following the initial cure, the laminates were postcured for eight hours in the autoclave at a temperature of 121°C. Upon completion of the postcure, each laminate was machined into six 38.1-mm by 280-mm tapered specimens. Each specimen was then tabbed and instrumented with strain gauges.

After the manufacturing process was completed, the dimensions of the specimens were measured. From these values the average ply thickness was determined to be 0.20 mm. In addition, strain gauges were placed along the centerline on the thick and thin sections approximately one specimen width from the tapered region. These gauges provided a far-field measurement of the modulus of the specimens. Little variation was seen within each specimen group as well as for all of the specimens tested. The measured moduli were 21.9 GPa in the thin section and 25.1 GPa in the thick section with coefficients of variation of 4.3 and 4.7%, respectively.

The specimens were tested under a quasistatic uniaxial tensile load in a servo-hydraulic testing machine. The specimens were loaded at a constant stroke rate of 0.635 mm/min. This is approximately equivalent to a strain rate of 5000 microstrain/min for a 127-mm test section.

The tests were halted several times to inspect visually for the onset of any delamination. Delamination was detected audibly during the loading of the specimen. A corresponding drop in load also occurred that indicated the increase of the compliance of the specimen. Whenever delamination was suspected, the test was halted and the specimen was examined. Black ink was applied to the edges of the still loaded specimen. If delamination had initiated, then the ink would be drawn inside. Using a light source from behind the specimen, the delaminated region could easily be seen within the specimen.

Of the six specimens cut from a given tapered laminate, the specimens from the edges often were significantly thinner and delaminated earlier than the average. Thus, the edge specimens are omitted from the reported averages.

Specimens: $[0_4/\pm 45_2]_s$

Delamination onset in these specimens is easily observed. The delamination event is accompanied by a loud cracking sound, and a fracture surface or crack appeared in the specimens. Additionally, a load drop is observed. The exact longitudinal location of the delamination initiation is difficult to determine due to the instability of the initial crack. In most cases, the delamination grew through the width and into the thin section of the specimen.

The delamination onset stress is determined by dividing the onset load by the measured cross-sectional area of the thin section of the specimen. The average delamination onset stress for specimens of the staircase ply drop sequence, 1, 2|3, 4|5, 6|, was 688 MPa. All of these specimens delaminated at the interface above the ply drops, the upper interface. In the specimens with an extended lower ply, 1, 2|3, 4|5|6|, the delamination strength increased by 4.2%. Half of these specimens delaminated in the upper interface, and half delaminated in the lower interface. The delamination strength does not appear to be a function of the initiation site. An increase of 16.2% in the delamination strength occurred in the specimens with an extended top ply, 1, 2|3, 4|6|5|. All but one of these specimens delaminated at the upper interface. In the last ply drop sequence, 6, 5|4, 3|2, 1|, the delamination strength decreased by 8.9%. These specimens delaminated above the ply drops.

Specimens: $[\pm 45_2/0_4]_s$

All of the specimens in this group delaminated at the interface below the ply drops. Significant delamination in these specimens was observed near the stress-free edges and in the thin section only. In most cases, the delamination did not extend into the thick section of the specimens. Delaminations originated near the root of the taper and moved in an unstable fashion into the thin section of the specimens. The ink placed on the sides of the specimens flowed into delaminated regions in the thin section of the specimens. Additionally, the delamination event was not as sudden of an event as observed in the $[0_4/\pm 45_2]_s$ specimens; however, a load drop was measured and used as the indication of the onset of damage. The delamination was accompanied by splitting of 0 deg core plies and fiber splintering at the edges.

Comparison and Discussion

The results from the finite element model are compared with the experimental evidence. The measured far-field moduli are close to those predicted either by laminated plate theory or by the finite element model (32.7 and 26.1 GPa, thin and thick sections, respectively). To determine the far-field stress when damage begins, the in situ strength of the resin layer is needed. Because interlaminar stresses are often singular in nature, a characteristic dimension is needed to apply a strength of materials failure criterion.[14,15] This dimension is used to indicate the point in the structure either at which the stress state is used as a point value or over which the stresses are averaged. Because the output of the finite element model is the average stress state of an element, the dimension assumed will be $1.0t_{ply}$, the longitudinal dimension of the elements at the ply drop.

Because the finite element model is linear, the analytical results are easily scaled. If the displacement is set so that the average far-field stress is equivalent to the experimentally observed damage onset stress, then the resulting maximum von Mises stress or principal shear stress may be considered as the in situ strength of the resin layer. This was done for all eight laminates and configurations using the results of the model with one and eight elements in the width, and the results are provided in Table 2. Consistent values from different configurations and stacking sequences would indicate a material constant, an accurate model, and an appropriate failure criterion. The two failure criteria employed, the von Mises stress and maximum principal shear stress, result in different values for the critical strength σ_0. In all cases, however, the scatter in the strength value is about the same with coefficients of variation of about 13–15%. If three specific specimen groups whose experimental values are judged to be in question are removed, then the corresponding average strengths are reduced and the coefficients of variation are reduced. For the model with only one element in the width, the coefficient of variation is reduced to about 7–8%. For the model with eight elements in the width, the coefficient of variation is reduced to below 5%.

The other differences between the two models are the locations of the elements with the critical stress. In all of the eight-element models, the critical element (von Mises stress) is located in the lower resin layer along the stress-free edge at the ply drop, as indicated by the circles in Fig. 8. This is independent of the stacking sequence. The one-element model predicts the critical location of the von Mises stress to be in the upper layer for the $[0_4/\pm 45_2]_s$ laminates and in the lower layer for the $[\pm 45_2/0_4]_s$ laminates. This difference is due to the high stress values at and near the free edges of the $-45/+45$ interface that are represented in the eight-element model.

Table 2 Critical applied stresses for damage onset

Laminate	Ply-drop configuration	One element: von Mises, σ_0	One element: Max. shear, σ_0	Eight elements: von Mises, σ_0	Eight elements: Max. shear, σ_0
$[0_4/\pm45_2]_s$	1, 2|3, 4|5, 6|[a]	157.5	170.4	192.5	220.8
	1, 2|3, 4|5|6|[a]	152.9	166.6	177.2	202.2
	1, 2|3, 4|6|5|[a]	166.0	187.8	175.7	201.0
	6, 5|4, 3|2, 1|	147.7	167.6	152.1	164.5
$[\pm45_2/0_4]_s$	1, 2|3, 4|5, 6|	220.2	249.6	233.1	264.1
	1, 2|3, 4|5|6|[a]	178.5	201.6	194.6	219.9
	1, 2|3, 4|6|5|[a]	177.6	197.6	182.3	208.8
	6, 5|4, 3|2, 1|	210.9	228.9	223.7	253.5
Average, all 8:		176.4	186.4	191.4	218.1
Coefficients of variation, %		(15.1)	(15.3)	(13.8)	(13.3)
Average[a]:		166.5	185.0	184.4	210.5
Coefficients of variation, %		(6.9)	(8.4)	(4.7)	(4.5)

[a]Specimen groups with experimental values judged to be consistent with analysis.

Table 3 Indicated and experimental far-field stresses at damage onset

Laminate	Ply-drop configuration	Predicted stress: von Mises, $\sigma_0 = 184$ MPa (% error)	Predicted stress: Max. shear, $\sigma_0 = 211$ MPa (% error)	Onset stress σ_f, MPa (coefficient of variation %)
$[0_4/\pm45_2]_s$	1, 2|3, 4|5, 6|	659 (−4.2)	656 (−4.7)	688 (3.91)
	1, 2|3, 4|5|6|	746 (4.1)	747 (4.1)	717 (5.23)
	1, 2|3, 4|6|5|	840 (5.0)	838 (4.7)	800 (5.45)
	6, 5|4, 3|2, 1|	760 (21.2)	756 (20.6)	627 (6.90)
$[\pm45_2/0_4]_s$	1, 2|3, 4|5, 6|	714 (−20.9)	720 (−20.3)	903 (4.70)
	1, 2|3, 4|5|6|	837 (−5.2)	845 (−4.3)	883 (1.86)
	1, 2|3, 4|6|5|	879 (1.2)	876 (0.8)	869 (6.70)
	6, 5|4, 3|2, 1|	744 (−17.6)	750 (−17.0)	903 (1.47)

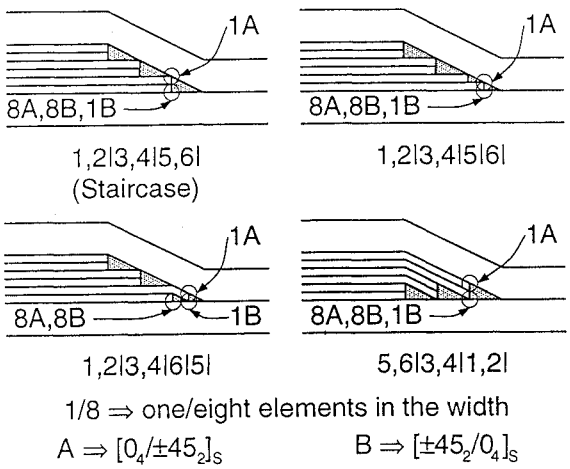

Fig. 8 Locations of critical von Mises stress.

Table 3 shows the results of an exercise in which the applied displacement at the thin section and, thus, the applied stress is scaled until the von Mises stress or maximum principal shear stress in the critical element reaches its respective strength value listed in Table 2. The strength values chosen are 184 MPa for the von Mises stress criterion and 211 MPa for the maximum principal shear stress criterion. Note that these are the average values obtained from the reduced data sets and the finite element model with eight elements in the width. In Table 3, the calculated far-field stress values are compared with experimental far-field stress values for all ply-drop configurations and laminate stacking sequences. As expected a reasonable agreement is observed on the average. Close agreement for individual cases would substantiate the use of the finite element model and the appropriate failure criterion. Because of the limited extent of the data and because three data sets are inconsistent with the present model, this exercise only suggests the feasibility of using the present finite element model and failure criteria to predict the onset of the observed failure mechanism.

The strength changes in the $[0_4/\pm45_2]_s$ laminates correspond well with those predicted by the finite element model, except for the 6, 5|4, 3|2, 1| ply-drop configuration that fails substantially lower than the predicted value. This may be due to manufacturing flaws. On the other hand, the $[\pm45_2/0_4]_s$ laminate with the standard staircase configuration failed substantially higher than the prediction. In this case, the initial onset of damage may have gone undetected.

The overall increase in strength of the $[\pm45_2/0_4]_s$ laminates compared with the $[0_4/\pm45_2]_s$ laminate corresponds well with that predicted by the finite element model. However, the observed trend within the $[\pm45_2/0_4]_s$ laminates does not agree with the tend predicted by the finite element model.

Conclusions

Tapered specimens with different ply-drop sequences were modeled, manufactured, and tested. The onset of delamination is controlled by the interlaminar stress states resulting from the taper and the stress-free edge. In all cases, the results of the finite element analysis show that altering the ply drop configuration decreases the stress state at the ply drop. This is experimentally validated by the 16% improvement in the damage onset stress of the $[0_4/\pm45_2]_s$ laminate with a 1, 2|3, 4|6|5| ply-drop configuration compared with the standard ply-drop configuration.

The approach suggested through the exercise of using the finite element model with an isotropic criteria applied to the interlaminar resin layer may provide a basis to predict the onset of damage near the root of a taper. This approach requires two parameters: the in situ strength of the resin layers and the appropriate dimension over which to average the stresses (the mesh size). In this study, the averaging dimension was chosen equal to the ply thickness, and the characteristic strength was empirically determined. Limited success was demonstrated in this exercise. Although the effect of changing the stacking sequence of the belt and core plies on damage onset was indicated by the finite element model, the effect of individual ply drop configurations was not as well indicated.

Structural tailoring of the ply-drop region can be an effective means to increase the structural integrity of tapered specimens.

Small alterations, although they do not alter the macroscopic elastic response of the component, can increase the strength. Care must be taken, however, to address the dominating failure mechanism both in choosing and in modeling the tailoring method.

Acknowledgments

This work was supported by the Army Research Office under Contract DAAG-29-83K0002. Robert Singleton and Thomas Doligalski were the contract monitors.

References

[1]O'Brien, T. K., "Interlaminar Fracture of Composites," NASA TM 85768, June 1984.

[2]O'Brien, T. K., "Characterization of Delamination Onset and Growth in a Composite Laminate," *Damage in Composite Materials*, ASTM STP 775, American Society for Testing and Materials, Philadelphia, PA, 1982, pp. 104–107.

[3]Kemp, B. L., and Johnson, E. R., "Response and Failure Analysis of a Graphite-Epoxy Laminate Containing Terminating Internal Plies," *Proceedings of the AIAA/ASME/ASCE/AHS 26th Structures, Structural Dynamics, and Materials Conference* (Orlando, FL), AIAA, New York, 1985, pp. 13–24.

[4]Curry, J. M., Johnson, E. R., and Starnes, J. H., Jr., "Effect of Dropped Plies on the Strength of Graphite Epoxy Laminates," *Proceedings of the AIAA/ASME/ASCE/AHS/ASC 29th Structures, Structural Dynamics and Materials Conference* (Monterey, CA), AIAA, Washington, DC, 1987, pp. 737–747.

[5]Fish, J. C., and Lee, S. W., "Delamination of Tapered Composite Structures," *Engineering Fracture Mechanics*, Vol. 34, No. 1, 1989, pp. 43–54.

[6]Salpekar, S. A., Raju, I. S., and O'Brien, T. K., "Strain Energy Release Rate Analysis of Delamination in a Tapered Laminate Subjected to Tension Load," *Proceedings of the American Society for Composites, 3rd Technical Conference* (Seattle, WA), Technomic, Lancaster, PA, 1988, pp. 642–654.

[7]Aramanios, E. A., and Parnas, L., "Delamination Analysis of Tapered Laminated Composites Under Tensile Loading," *Composite Materials: Fatigue and Fracture*, ASTM STP 1110, American Society for Testing and Materials, Philadelphia, PA, 1991, pp. 340–358.

[8]Murri, G. B., Salpekar, S. A., and O'Brien, T. K., "Fatigue Delamination Onset Prediction in Unidirectional Laminates," *Composite Materials: Fatigue and Fracture*, ASTM STP 1110, American Society for Testing and Materials, Philadelphia, PA, 1991, pp. 312–339.

[9]Chan, W. S., Rogers, C., Cronkhite, J. D., and Martin, J., "Delamination Control of Composite Rotor Hubs," *Journal of the American Helicopter Society*, Vol. 31, No. 3, 1986, pp. 60–69.

[10]Chan, W. S., "Delamination Arrester—An Adhesive Inner Layer in Laminated Composites," *Composite Materials: Fatigue and Fracture*, ASTM STP 907, American Society for Testing and Materials, Philadelphia, PA, 1986, pp. 176–196.

[11]Pogue, W. R., and Vizzini, A. J., "Structural Tailoring Techniques to Prevent Delamination in Composite Laminates," *Journal of the American Helicopter Society*, Vol. 35, No. 4, 1990, pp. 38–45.

[12]Llanos, A. S., and Vizzini, A. J., "The Effect of Film Adhesive on the Delamination Strength of Tapered Composites," *Journal of Composite Materials*, Vol. 26, No. 13, 1992, pp. 1968–1983.

[13]Fish, J. C., and Vizzini, A. J., "Tailoring Concepts for Improved Structural Performance of Rotorcraft Flexbeams," *Composites Engineering*, Vol. 2, Nos. 5–7, 1992, pp. 303–312.

[14]Whitney, J. M., and Nuismer, R. J., "Stress Fracture Criteria for Laminated Composites Containing Stress Concentrations," *Journal of Composite Materials*, Vol. 8, July 1974, pp. 253–265.

[15]Kim, R. Y., and Soni, S. R., "Experimental and Analytical Studies on the Onset of Delamination in Laminated Composites," *Journal of Composite Materials*, Vol. 18, Jan. 1984, pp. 70–80.